

A Novel and Robust Wavelet based Super Resolution Reconstruction of Low Resolution Images using Efficient Denoising and Adaptive Interpolation

Liyakathunisa

*Ph.D Research Scholar
Dept of Computer Science & Engg
S. J. College of Engineering
Mysore, India.*

liyakath@indiatimes.com

C.N .Ravi Kumar

*Professor & Head of Department
Dept of Computer Science & Engg
S. J. College of Engineering
Mysore, India.*

kumarcnr@yahoo.com

Abstract

High Resolution images can be reconstructed from several blurred, noisy and aliased low resolution images using a computational process know as super resolution reconstruction. Super resolution reconstruction is the process of combining several low resolution images into a single higher resolution image. In this paper we concentrate on a special case of super resolution problem where the wrap is composed of pure translation and rotation, the blur is space invariant and the noise is additive white Gaussian noise. Super resolution reconstruction consists of registration, restoration and interpolation phases. Once the Low resolution image are registered with respect to a reference frame then wavelet based restoration is performed to remove the blur and noise from the images, finally the images are interpolated using adaptive interpolation. We are proposing an efficient wavelet based denoising with adaptive interpolation for super resolution reconstruction. Under this frame work, the low resolution images are decomposed into many levels to obtain different frequency bands. Then our proposed novel soft thresholding technique is used to remove the noisy coefficients, by fixing optimum threshold value. In order to obtain an image of higher resolution we have proposed an adaptive interpolation technique. Our proposed wavelet based denoising with adaptive interpolation for super resolution reconstruction preserves the edges as well as smoothens the image without introducing artifacts. Experimental results show that the proposed approach has succeeded in obtaining a high-resolution image with a high PSNR, ISNR ratio and a good visual quality.

Keywords: Adaptive Interpolation, DWT, Denoising, Super Resolution, Thresholding.

1. INTRODUCTION

Super Resolution Reconstruction (SRR) is a process of producing a high spatial resolution image from one or more Low Resolution (LR) observation. It includes an alias free up sampling of the image thereby increasing the maximum spatial frequency and removing the degradations that arises during the image capture, Viz Blur and noise. An image is often corrupted by noise during acquisition and transmission. For instance in acquiring images with a CCD camera, light levels and sensor temperature are the major factors affecting the amount of noise in the resulting image. Images are also corrupted during transmission due to interference in the channel [3][6]. Viewing low resolution images limits many tasks, for example, one might have difficulty identifying, resolving or reading notices in front of a building, features or objects carried by someone in an image. Image quality is also limited by a sensors native resolution or other factors caused by under sampling images. Many low cost visible and thermal sensors spatially or electronically under sample an image. Under sampling results in aliased imagery in which the high frequency components are folded into low frequency components in the image, high frequency components is corrupted in these images[4].

Many approaches have been developed to increase image resolution, one of which uses 'micro dither' a special sensor or scanner captures multiple images, where each image is captured by displacing the sensor a known fraction of a pixel. The individual frames are combined into a higher resolution image [4]. An alternative approach employs super resolution image reconstruction, this software technology produces high resolution images using low cost, low resolution video equipment on the basis of a very small number of digital input frames, and resolution can be doubled or even quadrupled. Image quality can thus be improved using sensors without the need for hardware upgrades [4]. Super resolution reconstruction can increase image resolution without changing the design of optics and the detectors, by using a sequence of low resolution images.

Super resolution imaging has proved to be useful in many practical cases where multiple frames of the same scene are obtained. Some of the applications of super resolution imaging are for example in Astronomical imaging where it is possible to obtain different looks of the same scene, in satellite imagery when there is need to obtain higher resolution pictures than what is available, super-resolution imaging is a good choice. Medical imaging is a very important application area for image super-resolution, in medical imaging it is easier to obtain many different "looks" of the same scene with sub-pixel shifts in a controlled manner. CCD size limitations and shot noise prevents obtaining very high resolution images directly [3][5]. Super-resolution reconstruction can be used to get desired high resolution image.

The flow of the topics is as follows, In section II Mathematical Formulation for Super Resolution Model is created, section III presents Wavelet Transforms and Wavelet based Decomposition, section IV presents the proposed super resolution reconstruction of low resolution images, section V provides the proposed Super Resolution Reconstruction Algorithm, in VI simulation results and discussion of super resolution reconstruction is presented, and finally section VII consists of conclusion.

2. MATHEMATICAL FORMULATION FOR THE SUPER RESOLUTION MODEL

In this section we give the mathematical model for super resolution image reconstruction from a set of Low Resolution (LR) images. LR means that the pixel density with an image is less, offering fewer details. The CCD discretizes the images and produces a digitized noisy image. Imaging systems do not sample the scene according to Nyquist criterion. As a result of this the high frequency contents of images are destroyed and appear as LR.

In this section we give the mathematical model for super resolution image reconstruction from a set of Low Resolution (LR) images.

Let us consider the low resolution sensor plane by M_1 by M_2 . The low resolution intensity values are denoted as $\{y(i, j)\}$ where $i = 0 \dots M_1 - 1$ and $j = 0 \dots M_2 - 1$; if the down sampling parameters are

q_1 and q_2 in horizontal and vertical directions, then the high resolution image will be of size $q_1 M_1 \times q_2 M_2$. We assume that $q_1 = q_2 = q$ and therefore the desired high resolution image Z will have intensity values $\{z(k,l)\}$ where $k=0..qM_1-1$ and $l=0..qM_2-1$.

Given $\{z(k,l)\}$ the process of obtaining down sampled LR aliased image $\{y(i, j)\}$ is

$$y(i, j) = \frac{1}{q^2} \sum_{k=qi}^{(q+1)i-1} \sum_{l=qj}^{(q+1)j-1} z(k, l) \tag{1}$$

i.e. the low resolution intensity is the average of high resolution intensities over a neighborhood of q^2 pixels. We formally state the problem by casting it in a Low Resolution restoration frame work. There are P observed images $\{Y_m\}_{m=1}^P$ each of size $M_1 \times M_2$ which are decimated, blurred and noisy versions of a single high resolution image Z of size $N_1 \times N_2$ where $N_1 = qM_1$ and $N_2 = qM_2$.

After incorporating the blur matrix, and noise vector, the image formation model is written as

$$Y_m = H_m D Z + \eta_m \quad \text{Where } m=1..P \tag{2}$$

Here D is the decimation matrix of size $M_1 M_2 \times q^2 M_1 M_2$, H is PSF of size $M_1 M_2 \times M_1 M_2$, η_m is $M_1 M_2 \times 1$ noise vector and P is the number of low resolution observations Stacking P vector equations from different low resolution images into a single matrix vector

$$\begin{bmatrix} y_1 \\ \cdot \\ \cdot \\ y_p \end{bmatrix} = \begin{bmatrix} D H_1 \\ \cdot \\ \cdot \\ D H_p \end{bmatrix} Z + \begin{bmatrix} \eta_1 \\ \cdot \\ \cdot \\ \eta_p \end{bmatrix} \tag{3}$$

The matrix D represents filtering and down sampling process of dimensions $q^2 M_1 M_2 \times 1$ where q is the resolution enhancement factor in both directions. Under separability assumptions, the matrix D which transforms the $qM_1 \times qM_2$ high resolution image to $N_1 \times N_2$ low resolution images where $N_1 = qM_1$, $N_2 = qM_2$ is given by

$$D = D_1 \otimes D_1 \tag{4}$$

Where \otimes represents the kronecker product, and the matrix D_1 represents the one dimensional low pass filtering and down sampling. When $q=2$ the matrix D_1 will be given by

$$D_1 = \frac{1}{2} \begin{bmatrix} 11 & 00 & 00 & \dots & 00 \\ 00 & 11 & 00 & \dots & 00 \\ \vdots & \vdots & \vdots & \vdots & \vdots \\ 00 & 00 & 11 & & \end{bmatrix} \tag{5}$$

and

$$D = \frac{1}{2^2} \begin{bmatrix} 11 & 00 & 00 & \dots & 00 \\ 00 & 11 & 00 & \dots & 00 \\ \vdots & \vdots & \vdots & \ddots & \vdots \\ \vdots & \vdots & \vdots & \ddots & \vdots \\ 00 & 00 & & & 11 \end{bmatrix} \tag{6}$$

The square matrix H of dimensions $P_{N_1} \times P_{N_2}$ represents intra channel and inter channel blur operators. i.e. 2D convolution of channel with shift-invariant blurs. The blur matrix is of the form

$$H_I = \begin{bmatrix} H_{(0)} & H_{(1)} & \dots & H_{(M-1)} \\ H_{(M-1)} & H_{(0)} & \dots & H_{(M-2)} \\ \vdots & \vdots & \dots & \vdots \\ \vdots & \vdots & \dots & \vdots \\ H_{(1)} & H_{(2)} & \dots & H_{(0)} \end{bmatrix} \tag{7}$$

and it is circulant at the block level. In general each $H_{(i)}$ is an arbitrary $P_{M_1} \times P_{M_2}$, but if shift invariant circular convolution is assumed H(i) becomes

$$H_{(i)} = \begin{bmatrix} H_{(i,0)} & H_{(i,1)} & \dots & H_{(i,M-1)} \\ H_{(i,M-1)} & H_{(i,0)} & \dots & H_{(i,M-2)} \\ \vdots & \vdots & \dots & \vdots \\ \vdots & \vdots & \dots & \vdots \\ H_{(i,1)} & H_{(i,2)} & \dots & H_{(i,0)} \end{bmatrix} \tag{8}$$

which is also circulant at the block level $H_{(i,j)}$. Each $P \times P$ sub matrix (sub blocks) has the form.

$$H_{(i,j)} = \begin{bmatrix} H_{11(i,j)} & H_{12(i,j)} & \dots & H_{ip(i,j)} \\ H_{21(i,j)} & H_{22(i,j)} & \dots & H_{2p(i,j)} \\ \vdots & \vdots & \dots & \vdots \\ \vdots & \vdots & \dots & \vdots \\ H_{p1(i,j)} & H_{p2(i,j)} & \dots & H_{pp(i,j)} \end{bmatrix} \tag{9}$$

Where $H_{ii(m)}$ is intra channel blurring operator, $H_{ij(m)}^{i \neq j}$ is an inter channel blur i.e. $P \times P$ non circulant blocks are arranged in a circulant fashion, it's called Block Semi-Block Circulant (BSBC); which can be easily solved using blind deconvolution or regularization.

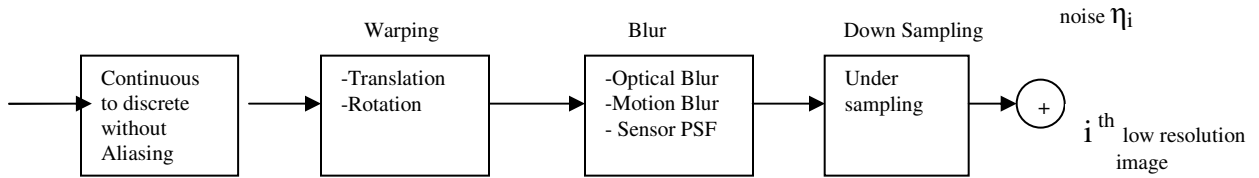


FIGURE1: Low Resolution Observation Model

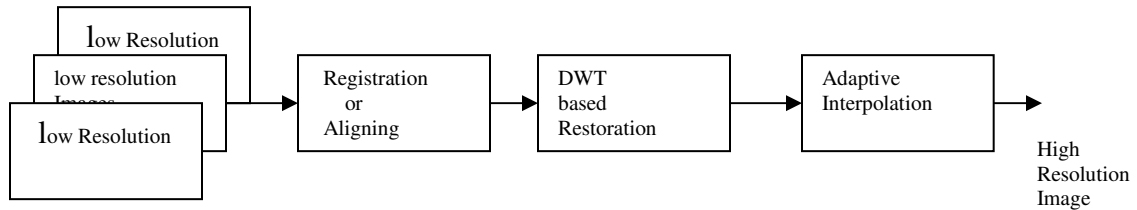


FIGURE 2: Super Resolution Reconstruction Model

3. Wavelet Transforms and Wavelet based Decomposition

Wavelet transforms decomposes a signal into a set of basis functions. Unlike Fourier transforms whose basis functions are sinusoids, wavelet transforms are based on small waves called wavelets of varying frequency and limited duration[6][7].

The Discrete wavelet transform of function $f(x,y)$ of size $M \times N$ is

$$W_{\phi}(j_0, m, n) = \frac{1}{\sqrt{MN}} \sum_{x=0}^{M-1} \sum_{y=0}^{N-1} f(x, y) \phi_{j_0, m, n}(x, y) \tag{10}$$

$$j \geq j_0$$

$$W_{\psi}^i(j, m, n) = \frac{1}{\sqrt{MN}} \sum_{x=0}^{M-1} \sum_{y=0}^{N-1} f(x, y) \psi_{j, m, n}^i(x, y) \quad i = \{H, V, D\} \tag{11}$$

j_0 is an arbitrary starting scale and $W_{\phi}(j_0, m, n)$ coefficients define an approximation of $f(x, y)$ at scale j_0 . The $W_{\psi}^i(j, m, n)$ coefficients add horizontal, vertical and diagonal details for scales $j \geq j_0$. Given the W_{ϕ} , W_{ψ}^i of Eq.10 and Eq.11, $f(x,y)$ is obtained via the inverse DWT.

$$f(x, y) = \frac{1}{\sqrt{MN}} \sum_{x=0}^{M-1} \sum_{y=0}^{N-1} W_{\phi}(j_0, m, n) \phi_{j_0, m, n}(x, y) + \frac{1}{\sqrt{MN}} \sum_{i=H, V, D} \sum_{j=0}^{\infty} W_{\psi}^i(j, m, n) \psi_{j, m, n}^i(x, y) \tag{12}$$

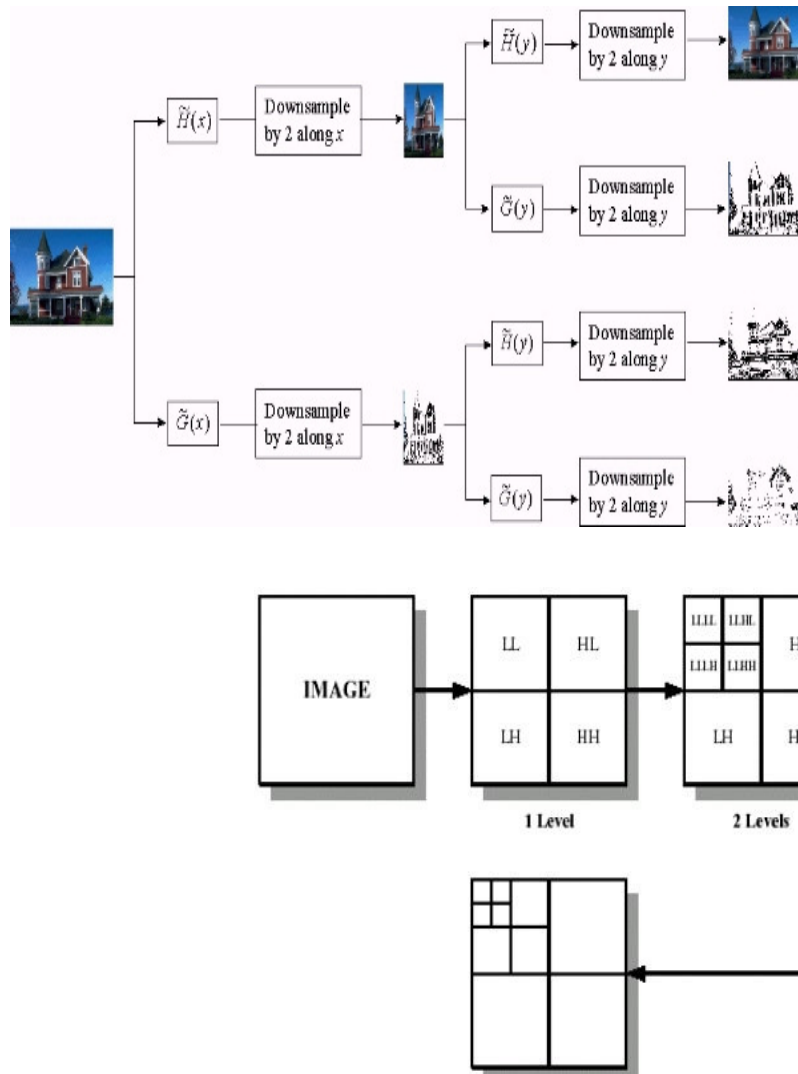


FIGURE 3: Discrete Wavelet Transformed down sampled image

The discrete wavelet transform uses low-pass and high-pass filters, $H(x)$ and $G(x)$, to expand a digital signal. They are referred to as analysis filters. These filters correspond to $\varphi(t)$ and $\psi(t)$ of Eq. 10. and Eq.11. The dilation performed for each scale is now achieved by a decimator. The coefficients c_k and d_k are produced by convolving the digital signal, with each filter, and then decimating the output. The c_k coefficients are produced by the low-pass filter, $H(x)$, and called coarse or approximate coefficients. The d_k coefficients are produced by the high-pass filter and called detail coefficients. Coarse coefficients provide information about low frequencies, and detail coefficients provide information about high frequencies. Coarse and detail coefficients are produced at multiple scales by iterating the process on the coarse coefficients of each scale. The entire process is computed using a tree-structured filter bank as shown in Fig.3.

The choice of filter depends on the type of applications we are using biorthogonal filter based wavelet transform. In biorthogonal case, there are two scaling functions which may generate different multiresolution analysis and accordingly two different wavelet functions.

4. Proposed Super Resolution Reconstruction of Low Resolution Images

The Low Resolution observation model of Eq. 2 is considered. The undersampled low resolution images are captured by natural jitter or some kind of controlled motion of the camera. Our proposed super resolution algorithms work in three phases: registration, restoration and interpolation.

4.1 Image Registration

For super resolution reconstruction, image registration is performed first in order to align the LR images as accurately as possible. It is a process of overlaying two or more images of the same scene taken at different times, from different view points and or by different sensors. Typically one image called the base image is considered the reference to which the other images called input images are compared. The objective is to bring the input image into alignment with the base image by applying a spatial transformation to the input image. Spatial transformation maps locations in one image into a new location in another image. Image registration is an inverse problem as it tries to estimate from sampled images Y_m , the transformation that occurred between the views Z_m considering the observation model of Eq 2. It is also dependent on the properties of the camera used for image acquisition like sampling rate (or resolution) of sensor, the imperfection of the lens that adds blur, and the noise of the device. As the resolution decreases, the local two dimensional structure of an image degrades and an exact registration of two low resolution images becomes increasingly difficult. Super resolution reconstruction requires a registration of high quality.

Different methods exist for estimating the motion or sub pixel shift between the two images[8]. The registration technique considered in our research is based on Fast Fourier Transform proposed by Fourier Mellin and DeCastro [9].

The transformation considered in our research is rotation, translation and shift estimation. Let us consider the translation estimation, the Fourier transform of the function is denoted by $F\{f(x, y)\}$ or $\hat{f}(w_x, w_y)$. The shift property of the Fourier transform is given by

$$F\{f(x+\Delta x, y+\Delta y)\} = \hat{f}(w_x, w_y) e^{i(w_x \Delta x + w_y \Delta y)} \quad (13)$$

Eq. 13 is the basis of the Fourier based translation estimation algorithms. Let $I_1(x, y)$ be the reference image and $I_2(x, y)$ is the translated version of the base image, i.e.

$$I_1(x, y) = I_2(x + \Delta x, y + \Delta y) \quad (14)$$

By applying the Fourier transform on both the sides of Eq. (14). We get

$$\hat{I}_1(w_x, w_y) = \hat{I}_2(w_x, w_y) e^{i(w_x \Delta x + w_y \Delta y)} \quad (15)$$

or equivalently,

$$\frac{\hat{I}_1(w_x, w_y)}{\hat{I}_2(w_x, w_y)} = e^{i(w_x \Delta x + w_y \Delta y)} \quad (16)$$

$$corr(x, y) \cong F^{-1} \left(\frac{\hat{I}_1(w_x, w_y)}{\hat{I}_2(w_x, w_y)} \right) = \delta(x + \Delta x, y + \Delta y) \quad (17)$$

For discrete images we replace the FT in the computation above with FFT, and $\delta(x + \Delta x, y + \Delta y)$ is replaced by a function that has dominant maximum at $(\Delta x, \Delta y)$ as

$$(\Delta x, \Delta y) = \arg \max \{corr(x, y)\} \quad (18)$$

Calculate the cross power spectrum by taking the complex conjugate of the second result. Multiplying the FT together element wise, and normalizing this product element wise.

$$corr(w_x, w_y) \cong \frac{\hat{I}_1(w_x, w_y)}{\hat{I}_2(w_x, w_y)} \bullet \left| \frac{\hat{I}_1(w_x, w_y)}{\hat{I}_2(w_x, w_y)} \right| \tag{19}$$

$$corr(w_x, w_y) = R \cong \frac{\hat{I}_1(w_x, w_y) \hat{I}_2^*(w_x, w_y)}{\left| \hat{I}_2(w_x, w_y) \right| \left| \hat{I}_1(w_x, w_y) \right|} = e^{i(w_x \Delta x + w_y \Delta y)} \tag{20}$$

where * denotes the complex conjugate. Obtain the normalized cross correlation by applying the inverse FT. i.e. $r = F^{-1}\{R\}$, determine the location of the peak in r. This location of the peak is exactly the displacement needed to register the images

$$(\Delta x, \Delta y) = \arg \max \{r\} \tag{21}$$

The angle of rotation is estimated by converting the Cartesian coordinates to log polar form. We observe that the sum of a cosine wave and a sine wave of the same frequency are equal to phase shifted cosine wave of the same frequency. That is if a function is written in Cartesian form as

$$v(t) = A \cos(t) + B \sin(t) \tag{22}$$

Then it may also be written in polar form as

$$v(t) = c \cos(t - \phi) \tag{23}$$

We may write the Eq (23) in polar form as

$$Y = y(x) = \frac{a_0}{2} + \sum_{k=1}^N m_k \cos(2\pi f_k x - \phi_k) \tag{24}$$

Where

$$m_k = \sqrt{a_k^2 + b_k^2} \dots (\text{magnitude}) \tag{25}$$

$$\phi_k = \tan^{-1} \left(\frac{b_k}{a_k} \right) \dots (\text{Phase})$$

The Shift is estimated by finding cross power spectrum and computing Eq. (20). We obtain the normalized cross correlation by applying the inverse FT. i.e. $r = F^{-1}\{R_2\}$, determines the location of the peak in r. This location of the peak is exactly the shift $I(x_0, y_0)$ needed to register the images. Once we estimated the angle of rotation and translation and shift, a new image is constructed by reversing the angle of rotation, translation and shift.



FIGURE 4: Registered Image

In the second phase the low resolution registered images are fused using fusion rule, then restoration is performed using our proposed novel denoising technique. In the final phase proposed adaptive interpolation is performed to obtain an image with double, quadrupled the resolution of the original.

4.2 Wavelet based Restoration

Images are obtained in areas ranging from everyday photography to astronomy, remote sensing, medical imaging and microscopy. In each case there is an underlying object or scene we wish to observe, the original or the true image is the ideal representation of the observed scene. Yet the observation process is never perfect, there is uncertainty in the measurement occurring as blur, noise and other degradations in the recorded images. Image restoration aims to recover an estimate of the original image from the degraded observations. Classical image restoration seeks an estimate of the true image assuming the blur is known, whereas blind image restoration tackles the much more difficult but realistic problem where the degradations are unknown.

The low resolution observation model of Eq.2 is considered. We formally state by casting the problem in multi channel restoration format, the blur is considered as between channels and within channel of the low resolution images. In order to remove the blur and noise from the LR images, we have proposed an efficient wavelet based denoising using thresholding, our proposed approach performs much better when compared to other approaches.

4.2.1. Proposed Efficient wavelet based Denoising for SRR using Thresholding

Image denoising techniques are necessary to remove random additive noises while retaining as much as possible the important image features. The main objective of these types of random noise removal is to suppress the noise while preserving the original image details [6]. Statistical filter like average filter, wiener filter can be used for removing such noises but wavelet based denoising techniques proved better results than these filters. The wavelet transforms compresses the essential information in an image into a relatively few, large coefficients which represents image details at different resolution scales. In recent years there has been a fair amount of research on wavelet thresholding and threshold selection for image denoising [10] [11] [12].

Let Z be an $M \times M$ image from Eq. (2), during transmission the image Z is corrupted by zero mean white Gaussian noise η with standard deviation σ . At the receiver end the noisy observation Y of Eq. (2) is obtained. The goal is to obtain the image Z from noisy observation Y such that the MSE is minimum. Wavelet Transforms decomposes the image into different frequency subbands. Small coefficients in the subbands are dominated by noise while coefficients with large absolute value carry more image information than noise. Replacing noisy coefficients by zeros and an inverse wavelet transform may lead to reconstruction that has lesser noise. Normally hard thresholding and soft thresholding techniques are used for denoising.

Hard Thresholding

$$D(X, T) = \begin{cases} X & \text{if } |X| > T \\ 0 & \text{if } |X| < T \end{cases} \quad (26)$$

Soft Thresholding

$$D(X, T) = \text{Sign}(X) * \max(0, |X| - T) \quad (27)$$

Where X is the input subband, D is the denoised band after thresholding and T is the threshold level. The denoising algorithms which are based on thresholding suggests, that each coefficient of every detail subband is compared to threshold level and is either retained or killed if its magnitude is greater or less respectively.

In wavelet decomposition of an image we obtain one approximate (LL) and three details (LH, HL and HH) subbands. The approximate coefficients are not submitted in this process. Since on one

hand they carry the most important information about the image, on the other hand the noise mostly affects the high frequency subbands. Hence the HH subband contains mainly noise. For estimating the noise level we use the Median Absolute Deviation (MAD) as proposed by Donoho [13].

$$\sigma = \frac{\text{Median} |Y_{ij}|}{0.6745}, Y_{ij} \in LH, HL, HH \tag{28}$$

The factor 0.6745 in the denominator rescales the numerator, so that σ is also a suitable estimator for standard deviation for Gaussian white noise.

Selecting an optimum threshold value (T) for soft thresholding is not an easy task. An optimum threshold value should be selected based on the subband characteristics. In wavelet subbands as the level increases, the coefficients of the subband become smoother. For example when an image is decomposed into 2 level DWT using Daubechies 4 tap or bio-orthogonal wavelet transform, we get 8 subbands Fig.3, the HH subband of first level contains large amount of noise, hence the noise level is estimated for the HH subband of level1 using equation (28).Once the noise level is estimated, we select the threshold value T. The Threshold value T is

$$T = \sigma - (|HM - GM|) \tag{29}$$

Here σ is the noise variance of the corrupted image. As given in [6], the Harmonic mean and geometric mean are best suited for the removal of Gaussian noise, hence we use the absolute difference of both the Harmonic Mean (HM) and Geometric Mean (GM) or either of the means can also be considered for denoising the image corrupted by Gaussian noise. The harmonic mean filter is better at removing Gaussian type noise and preserving edge features than the arithmetic mean filter. Hence we have considered harmonic mean than arithmetic mean. The process is repeated for LH and HL bands and threshold is selected for all the three bands once threshold is estimated, soft thresholding of Eq.27, is performed to denoise the image.

$$HM = \frac{M^2}{\sum_{i=1}^M \sum_{j=1}^M \frac{1}{g(i,j)}} \tag{30}$$

$$GM = \left[\prod_{i=1}^M \prod_{j=1}^M g(i,j) \right]^{\frac{1}{M^2}} \tag{31}$$

4.3. Proposed Adaptive Interpolation for Super Resolution reconstruction

The algorithm works in four phases: In the first phase the wavelet based fused image is expanded. Suppose the size of the fused image is n x m. The image will be expanded to size N (2n-1) x (2m-1). In the Fig.5 solid circles show original pixels and hallow circles show undefined pixels. In the remaining three phases these undefined pixels will be filled

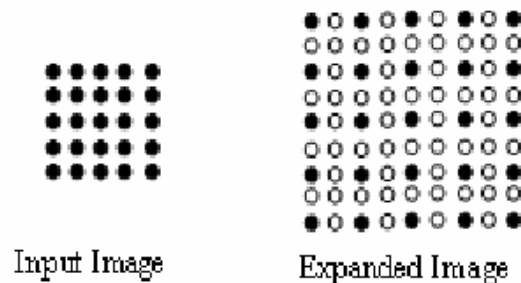


FIGURE 5 : High Resolution Grid

The second phase of the algorithm is most important one. In this phase the interpolator assigns value to the undefined pixels

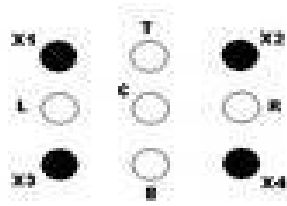


FIGURE 6: HR unit cell with undefined pixels Top, Center, Bottom, Left, Right denoted by T,C,B,L,R.

The undefined pixels are filled by following mutual exclusive condition.

Uniformity: select the range (X_1, X_2, X_3, X_4) and a Threshold T.

if range $(X_1, X_2, X_3, X_4) < T$ Then

$$C = \frac{(X_1 + X_2 + X_3 + X_4)}{4} \tag{32}$$

if there is edge in NW-SE Then

$$C = (X_1 + X_2) / 2$$

if there is edge in NS Then

$$T = (X_1 + X_2) / 2 \text{ and } B = (X_3 + X_4) / 2$$

if there is edge in EW Then

$$L = (X_1 + X_3) / 2 \text{ and } R = (X_2 + X_4) / 2 \tag{33}$$

In this phase, approximately 85% of the undefined pixels of HR image are filled. In the third phase the algorithm scans the magnified image line by line, looking for those pixels which are left undefined in the previous phase.

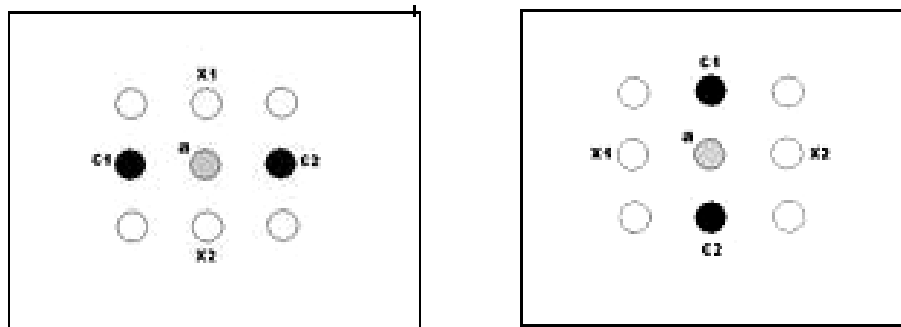


FIGURE 7 : Layout referred in the phase 3

In the third phase ,the algorithm checks for the layout as shown in Figure(7).

$$\begin{aligned} & \text{if there is edge } c_1 c_2 \text{ then } a = (c_1 + c_2) / 2 \\ & \text{else if there is edge } X_1 X_2 \text{ then } a = (X_1 + X_2) / 2 \end{aligned} \quad (34)$$

In the fourth phase all the undefined pixels will be filled. If there are any undefined pixels left then the median of the neighboring pixels is calculated and assigned. We call our interpolation method adaptive as the interpolator selects and assigns the values for the undefined pixels based on mutual exclusive condition.

5. Proposed Algorithm for Super Resolution Reconstruction of Low Resolution Images.

Our proposed novel super resolution reconstruction consists of following consecutive steps:

Step 1: Three input low resolution blurred, noisy, under sampled, rotated, shifted images are considered.

$$\text{i.e. } I_1(i, j), I_2(i, j), I_3(i, j) \text{ where } i=1 \dots N, j=1 \dots N \quad (35)$$

Step 2: The images are first preprocessed, i.e. registered using FFT based algorithm, as explained in section(4.1).

Step 3: The registered low resolution images are decomposed using DWT to a specified number of levels. At each level we will have one approximation i.e. LL sub band and 3 detail sub bands, i.e. LH, HL, HH coefficients.

Step 4: The decomposed images are fused using the fusion rule i.e. Maximum Frequency Fusion: "fusion by averaging for each band of decomposition and for each channel the wavelets coefficients of the three images is averaged". That is maximum frequencies of approximate and detail coefficients are fused separately

$$A_j^o I = \max(A_j^o I_1 + A_j^o I_2 + A_j^o I_3) / 3 \quad D_j^d I = \max(D_j^d I_1 + D_j^d I_2 + D_j^d I_3) / 3 \quad (36)$$

Step 5: The fused image contains LL, LH, HL and HH subbands.

- a) Obtain the noise variance (σ) using Eq.(28) for LH, HL and HH subbands of level one.
- b) Compute Eq. (29) and select the threshold (T) for LH, HL and HH subbands of level 1.
- c) Denoise all the detail subband coefficients of level one (except LL) using soft thresholding given in Eq. (27) by substituting the threshold value obtained in step (5b).

Step 6: Most of the additive noise will be eliminated during the fusion process by denoising using our proposed soft thresholding approach as explained in section (4.2.1), where as the image is deblurred using Iterative Blind Deconvolution Algorithm (IBD)[14].

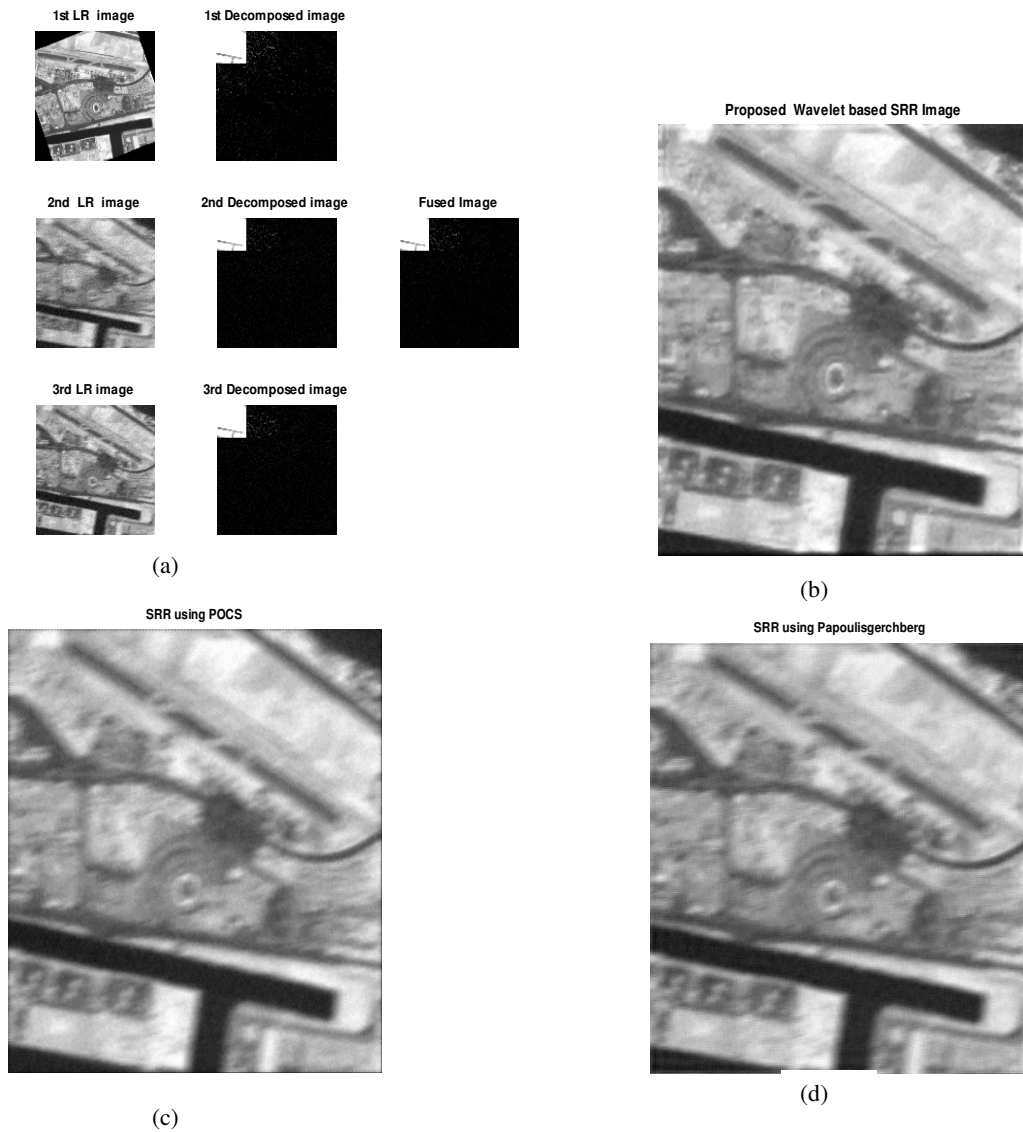
Step 8: Inverse DWT is applied to obtain a high resolution restored image.

Step 9: Finally in order to obtain a super resolved image, an image with double the resolution as that of the original image, our proposed adaptive interpolation as explained in section (4.3) is applied.

6. Simulation Results and Discussions

In computer simulations, three LR (256x 256) images are considered. We have tested using both motion blur with an angle of (10, 20 and 30) and Gaussian blur of 3x3, 5x5 and 7x7 is considered. Gaussian white noise with SNR (5, 10,15 and 20 dB) is added to the blurred low resolution images. A Super Resolution image of size 512 x512 and 1024x1024 is reconstructed from three noisy, blurred, under sampled, mis-registered images

Case 1: Abudabi SAR grayscale Low resolution Images with a Super resolution factor of 2 (enlarged from 256x256 to 512 by 512)



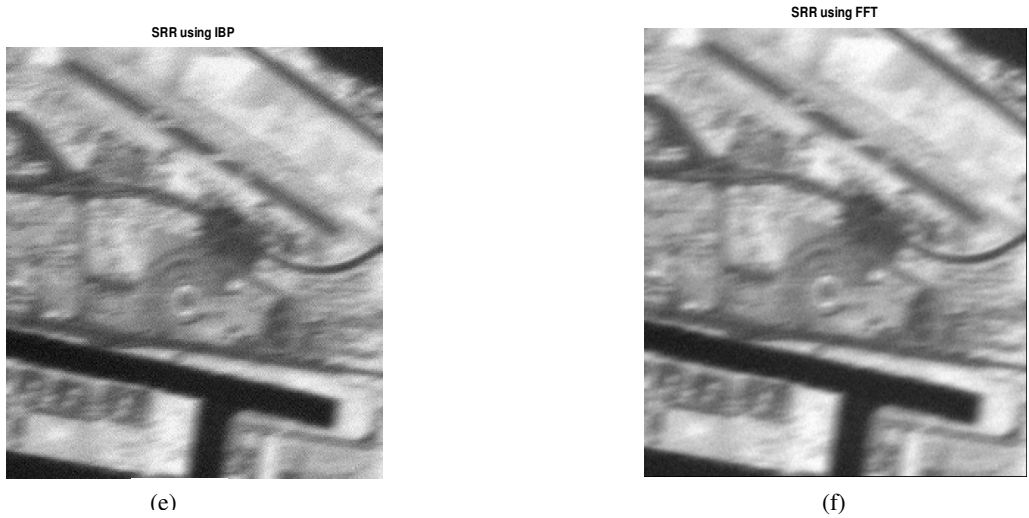
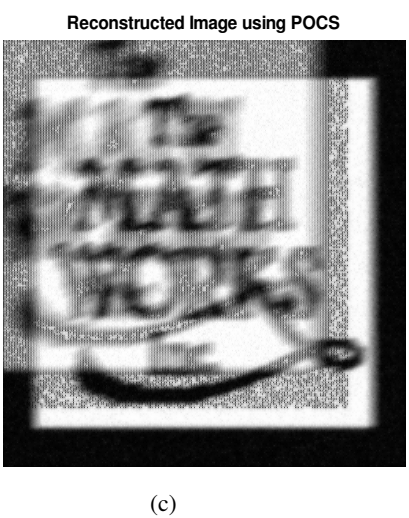
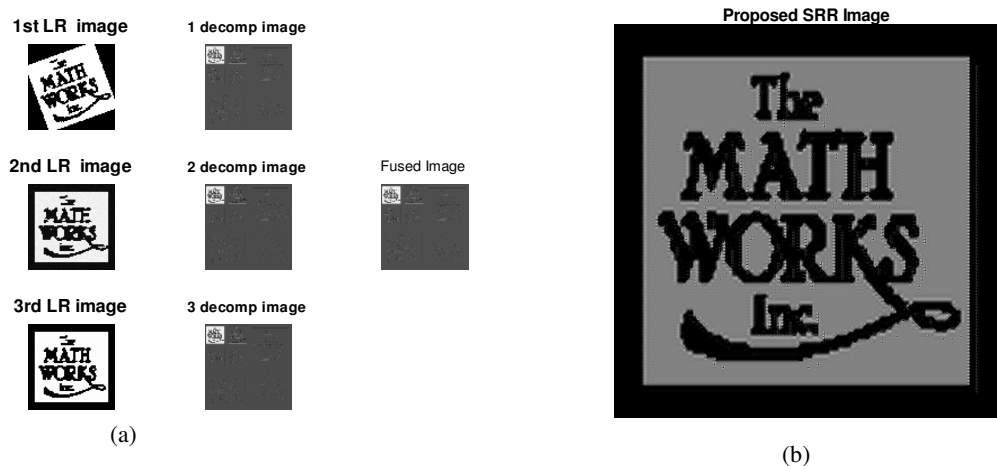


FIGURE 8: (a) Low Resolution Images (b) Proposed wavelet SRR (c) Projection on to Convex Sets(POCS) SRR (d) Papoulis Gerchberg SRR (e) Iterative Back Propagation (IBP) SRR (f) FFT based SRR
 Case 2: Logo grayscale Low resolution Images with a Super resolution factor of 4 (enlarged from 128x128 to 512 by 512)



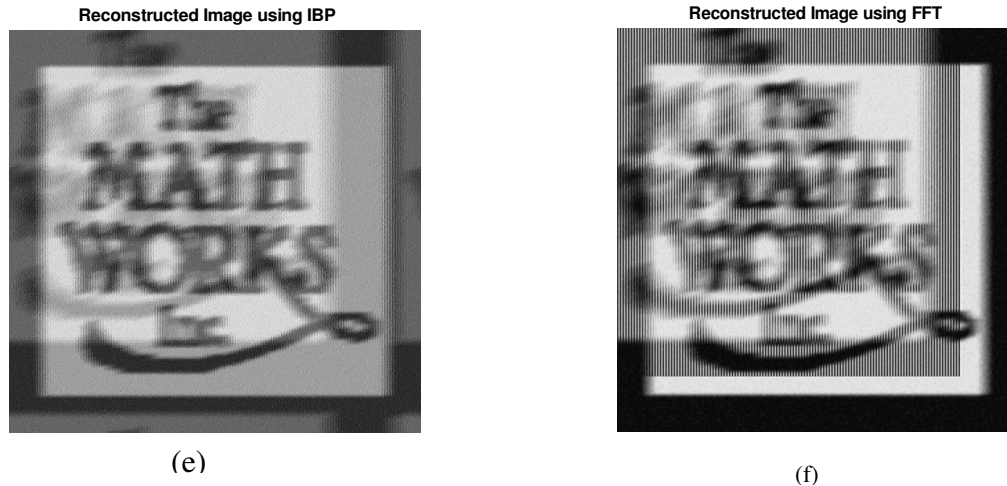


FIGURE 9: (a) Low Resolution Images (b) Proposed wavelet SRR (c) Projection on to Convex Sets (POCS) SRR (d) Papoulis Gerchberg SRR (e) Iterative Back Propagation (IBP) SRR (f) FFT based SRR

Simulations are carried out to verify noise and blur removing capability of the proposed super resolution reconstruction and the results are compared with several existing state of art techniques. A quantitative comparison is performed between proposed wavelet based super reconstruction and several existing techniques in terms of Improvement in Signal to Noise Ratio (ISNR), Peak Signal to Noise ratio (PSNR), Mean Square Error (MSE), Super Resolution Factor (SRF) and Mean Structural Similarity (MSSIM) Index. Our method produced results superior to other methods in both visual image quality and quantitative measure. Simulations were made on several gray scale and color images corrupted with Gaussian noise and motion blur.

The performance of the algorithm for various images at different blur and noise levels is studied and the results for two cases are shown in Fig.8. and Fig 9. The quantities for comparison are defined as follows and Table I and II display the quantitative measures.

1) Improvement in Signal-to-Noise Ratio (ISNR)

For the purpose of objectively testing the performance of the restored image, Improvement in signal to noise ratio (ISNR) is used as the criteria which is defined by

$$ISNR = 10 \log_{10} \frac{\sum_{i,j} [f(i, j) - y(i, j)]^2}{\sum_{i,j} [f(i, j) - g(i, j)]^2} \tag{37}$$

Where j and i are the total number of pixels in the horizontal and vertical dimensions of the image; f(i, j), y(i, j) and g(i, j) are the original, degraded and the restored image.

2) The MSE and PSNR of the reconstructed image is

$$MSE = \frac{\sum [f(i, j) - F(I, J)]^2}{N^2} \tag{38}$$

Where f(i, j) is the source image F(I, J) is the reconstructed image, which contains N x N pixels

$$PSNR = 20 \log_{10} \left(\frac{255}{RMSE} \right) \quad (39)$$

3) Super Resolution Factor

$$SRF = \frac{\sum_{i=1}^M \sum_{j=1}^N (F(i, j) - f(i, j))^2}{\sum_{i=1}^M \sum_{j=1}^N (y(i, j) - f(i, j))^2} \quad (40)$$

4) MSSIM

The structural similarity (SSIM) index is defined in [29] by equations

$$SSIM(f, F) = \frac{(2\mu_f \mu_F + C_1)(2\sigma_f + C_2)}{(\mu_f^2 + \mu_F^2 + C_1)(\sigma_f^2 + \sigma_F^2 + C_2)} \quad (41)$$

$$MSSIM(f, F) = \frac{1}{G} \sum_{p=1}^G SSIM(f, F) \quad (42)$$

The Structural SIMilarity index between the original image and reconstructed image is given by SSIM, where μ_f and μ_F are mean intensities of original and reconstructed images, σ_f and σ_F are standard deviations of original and reconstructed images, f and F are image contents of p th local window and G is the number of local windows in the image.

The simulation results show that our approach provides a visually appealing output. The proposed wavelet based super resolution reconstruction with efficient denoising can reconstruct a super resolution image from a series of blurred, noisy, aliased and downsampled low resolution images, which is demonstrated by two cases as show in Fig. 8 and Fig.9.

In case 1, Fig 8, three LR SAR images of Abu Dhabi stadium are considered which are corrupted by Gaussian noise of standard deviation ($\sigma = 10, 15$ & 20) and motion blur of angle ($10, 20$ & 30). The results of the proposed SRR are compared with Projection on to Convex Sets (POCS)[21], Papoulis Gerchberg algorithm [23] [24], Iterative Back Propagation (IBP) [22] and FFT based SRR [26] [27].

Table I and II gives the quantitative measures of abudhabi.gif, logo.tif, lean.jpg and baboob.png images. Fig10, a, b, c & d shows the comparison graph of various quantitative measures for the LR test images. When compared with standard state of art techniques, it is clear that the proposed wavelet based SRR with efficient denoising and adaptive interpolation can eliminate the noise and blur while preserving the edges and fine details, and can reconstruct a super resolution image with a super resolution factor of 2, 4 times than the original image.

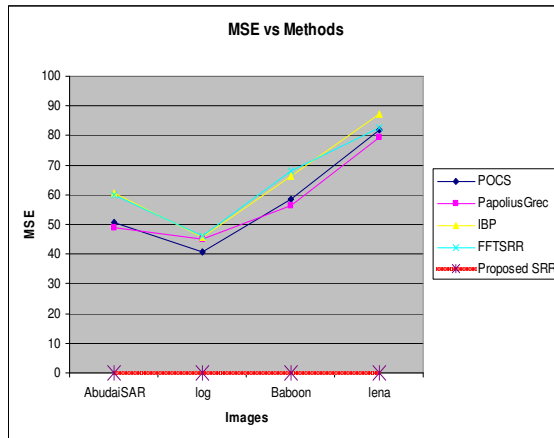
The results show that fig 8b and 9b has more sharp edges and less noise when compared to state of art techniques.

Table I: MSE and PSNR comparison of our proposed approach with other approaches

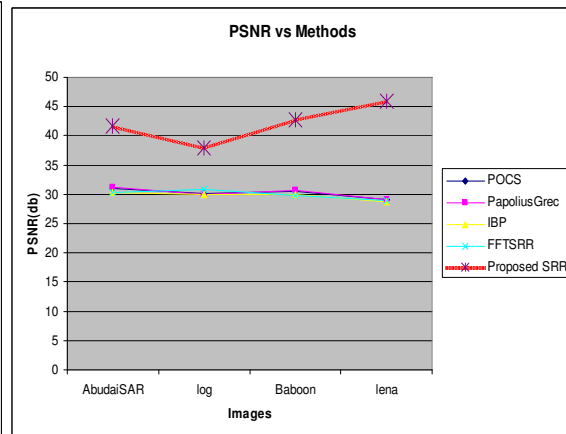
Source Image	POCS		Paploius Greberg		IBP		FFT SRR		Proposed Wavelet SRR	
	MSE	PSNR	MSE	PSNR	MSE	PSNR	MSE	PSNR	MSE	PSNR
AbudaiSAR	50.62	31.08	48.9	31.23	60.51	30.31	59.83	30.36	0.002	41.74
log	40.63	30.06	45.1	30.04	45.78	29.95	46.08	30.86	0.035	37.87
Baboon	58.64	30.44	56.28	30.62	66.46	29.9	68.04	29.8	0.086	42.8
lena	82.015	28.99	79.52	29.12	87.21	28.72	82.48	28.96	0.061	45.95

Table II: ISNR and MSSIM comparison of our proposed approach with other approaches

Source Image	POCS		Paploius Greberg		IBP		FFT SRR		Proposed Wavelet SRR	
	ISNR	MSSIM	ISNR	MSSIM	ISNR	MSSIM	ISNR	MSSIM	ISNR	MSSIM
AbudaiSAR	3.392	0.6783	3.96	0.625	3.35	0.761	3.39	0.68	6.49	0.833
log	3.58	0.723	4.61	0.76	3.69	0.79	3.94	0.73	5.05	0.871
Baboon	2.8	0.671	3.09	0.663	2.13	0.711	2.51	0.702	6.87	0.778
lena	3.58	0.683	3.43	0.617	3.04	0.786	4.08	0.711	6.01	0.858



(a)



(b)

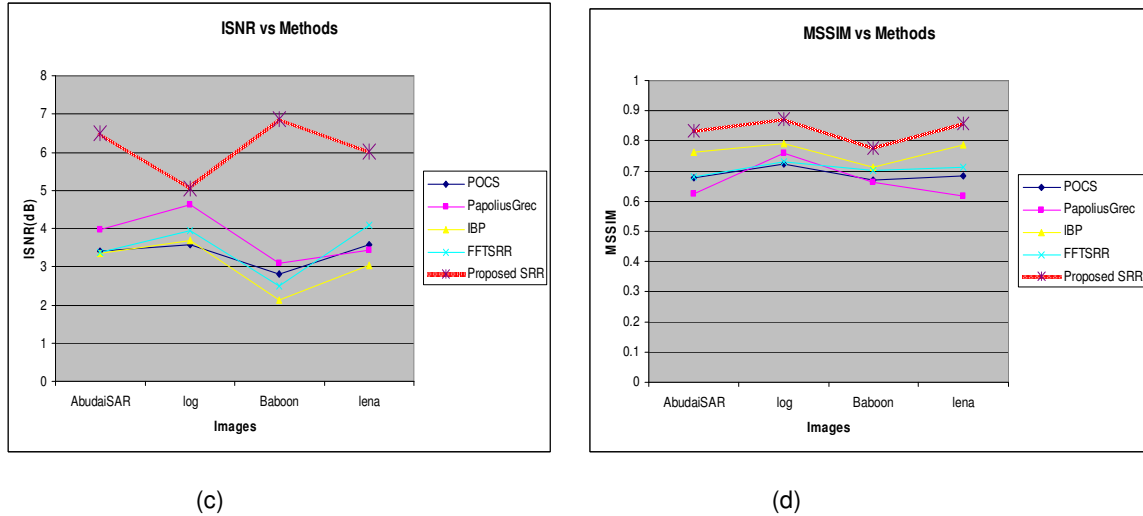


Figure 10: (a) Comparison graph of MSE at different Blur and noise densities of LR images (b) Comparison graph of PSNR at different Blur and noise densities of LR images. (c) Comparison graph of ISNR at different Blur and noise densities of LR images (d) Comparison graph of MSSIM at different Blur and noise densities of LR images

7. CONCLUSION

In this paper we have proposed a novel and robust wavelet based super resolution reconstruction of low resolution images using efficient denoising and adaptive interpolation. Wavelet transforms are suitable for achieving a high super resolution reconstruction image. The proposed wavelet based denoising is based on threshold estimation and analysis of statistical parameters like harmonic mean, geometric mean and standard deviation of the detail sub band coefficients. Harmonic mean filter performs better when compared to arithmetic mean filters and preserve the edges which are most significant for super resolution reconstruction. Experiments are conducted on different natural images corrupted by various noise levels to access the performance of the proposed thresholding method in comparison with other methods. The advantage of using wavelets and adaptive interpolation for super resolution reconstruction is blocking artifacts are reduced and we are able to obtain very high PSNR and ISNR value when compared to the state of art super resolution reconstruction. With our proposed Adaptive interpolation technique we are able to obtain a very high super resolution image with super resolution factor of 2, 4 times than that of the original image. Experimental results show that our proposed method performs quite well in terms of robustness and efficiency.

REFERENCES

- [1] Liyakathunisa and C.N.Ravi Kumar "Advances in Super Resolution Reconstruction of Low Resolution Images" International Journal of Computational Intelligence Research ISSN 0973-1873 Volume 6, Number 2 (2010), pp. 215–236.
- [2] Liyakathunisa, C.N.Ravi Kumar and V.K. Ananthashayana , "Super Resolution Reconstruction of Low Resolution Images using Wavelet Lifting schemes" in Proc ICCEE'09, " 2nd International Conference on Electrical & Computer Engineering", Dec 28-30TH 2009, Dubai, Indexed in IEEE Xplore.
- [3] S. Chaudhuri, Ed., Super-Resolution Imaging. Norwell, A: Kulwer, 2001.
- [4] S.Susan Young, Ronal G.Diggers, Eddie L.Jacobs, "Signal Processing and performance Analysis for imaging Systems", ARTEC HOUSE, INC 2008
- [5] S. C. Park, M. K. Park, and M. G. Kang, "Super-resolution image reconstruction: A technical review," IEEE Signal Processing Mag., vol. 20, pp. 21–36, May 2003.
- [6] Gonzalez Woods, "Digital Image Processing", 2nd Edition.
- [7] A. Jensen, A.Ja Cour-Hardo, "Ripples in Mathematics" Springer publications.
- [8] Barbara Zitova, J.Flusser, "Image Registration: Survey", Image and vision computing, 21, Elsevier publications, 2003.

- [9] E.D. Castro, C. Morandi, Registration of translated and rotated images using finite Fourier transform, IEEE Transactions on Pattern Analysis and Machine Intelligence (1987) 700–703.
- [10] S. Grace Chang, Bin Yu and M. Vattereli. (2000). Adaptive Wavelet Thresholding for Image denoising and compression IEEE Transaction, Image Processing, vol. 9, pp. 1532-15460.
- [11] S.K.Mohiden, Perumal, Satik, "Image Denoising using DWT", IJCSNS, Vol 8, No 1, 2008.
- [12] D. Gnanadurai, V.Sadsivam, "An Efficient Adaptive Thresholding Technique for Wavelet based Image Denoising" IJSP, Vol 2, spring 2006.
- [13] D.L. Donoho and I.M John Stone (1995), Adapting to unknown smoothness via wavelet shrinkage, Journal of American Association, Vol 90, no, 432, pp1200-1224 .
- [14] Grayer and J.C. Danity, "Iterative Blind Deconvolution", July 1988, vol13, No 7, optics letters
- [15] G. Nason, "Choice of the threshold parameter in wavelet function estimation," in Wavelets in Statistics, A. Antoniadis and G. Oppenheim, Eds. Berlin, Germany: Springer-Verlag, 1995.
- [16] Le Moigne J. and Cromp R. F., 1996, "The use of wavelets for remote sensing image registration and fusion". Technical Report TR-96-171, NASA Goddard Space Flight Center.
- [17] I. M. Johnstone and B.W. Silverman, "Wavelet threshold estimators for data with correlated noise," J. R. Statist. Soc., vol. 59, 1997.
- [18] D. L. Donoho, "De-noising by soft-thresholding," IEEE Trans. Inform. Theory, vol. 41, pp. 613–627, May 1995
- [19] H. H. Wang, "A new multi wavelet-based approach to image fusion", Journal of Mathematical Imaging and Vision, vol.21, pp.177-192, Sep 2004
- [20] S. Borman and R.L. Stevenson, "Super-resolution from Image sequences -A Review", in Proc. 1998 Midwest Symp. Circuits and Systems, 1999, pp.374-378.
- [21] A.M. Tekalp, M.K. Ozkan, and M.I. Sezan, "High-resolution image reconstruction from lower-resolution image sequences and space varying image restoration," in Proc. IEEE Int. Conf. Acoustics, Speech and Signal Processing (ICASSP), San Francisco, CA., vol. 3, Mar. 1992, pp. 169-172
- [22] M. Irani and S. Peleg, "Improving resolution by image registration," CVGIP: Graphical Models and Image Proc., vol. 53, pp. 231-239, May 1991.
- [23] Papoulis, A. (1975) A new algorithm in spectral analysis and band-limited extrapolation. IEEE Transactions on Circuits and Systems, CAS-22, 735–742.
- [24] Gerchberg, R. (1974) Super-resolution through error energy reduction. Optical Acta, 21, 709–720.
- [25] Priyam chatterjee, Sujata Mukherjee, Subasis Chaudhuri and Guna Setharaman, "Application of Papoulis – Gerchberg Method in Image Super Resolution and inpainting," The Computer Journal Vol 00 No 0, 2007.
- [26] P. Vandewalle, S. Susstrunk, and M. Vetterli, Lcav, "A frequency domain approach to registration of aliased images with application to Super resolution", EURASIP Journal on applied signal processing pp 1-14, 2006.
- [27] Deepesh Jain, " Super Resolution Reconstruction using Papoulis-Gerchberg Algorithm" EE392J – Digital Video Processing, Stanford University, Stanford, CA
- [28] F. Sroubek, G. Cristobal and J. Flusser, "Simultaneous Super Resolution and Blind deconvolution ", Journal of Physics: Conference series 124(2008) 01204
- [29] Freeman, W. T., Jones, T. R., and Pasztor, E. C. Example-based super-resolution, IEEE Computer Graphics and Applications, 22, 56–65, 2000.
- [30] S. Baker and T. Kanade, "Limits on Super Resolution and How to Break Them ", Proc. IEEE conf. Computer Vision and Pattern Recognition, 2000.
- [31] S. Lertrattanapanich and N. K. Bose, "High Resolution Image Formation from Low Resolution Frames Using Delaunay Triangulation", IEEE Trans on image processing vol. 11, no. 12, December 2002.
- [32] R.Y. Tsai and T.S. Huang, "Multiple frame image restoration and registration," in Advances in Computer Vision and Image Processing. Greenwich, CT: AI Press Inc., 1984, pp. 317-339.
- [33] Wang, Bovik, Sheikh, et al. "Image Quality Assessment: From Error Visibility to Structural Similarity," IEEE Transactions of Image Processing, vol. 13, pp. 1-12, April 2004.
- [34] S. Mallat, "A theory for multiresolution signal decomposition: The wavelet representation," IEEE Trans. Pattern Anal. Machine Intell, vol. 11, pp. 674–693, July 1989.
- [35] X. Li and M. T. Orchard, "New Edge-Directed Interpolation," IEEE Trans. on Image Processing, vol. 10, no. 10, October 2001.
- [36] J.W. Hwang and H.S. Lee, "Adaptive Image Interpolation Based on Local Gradient Features," IEEE Signal Processing Letters, vol. 11, no. 3, March 2004.
- [37] S. Carrato and L. Tenze, "A High Quality 2x Image Interpolator," IEEE Signal Processing Letter, vol. 7, no. 6, June 2000.
- [38] T. Acharya, P.S. Tsai, "Image up-sampling using Discrete Wavelet Transform," in Proceedings of the 7th International Conference on Computer Vision, Pattern Recognition and Image Processing (CVPRIP 2006), in conjunction with 9th Joint Conference on Information Sciences (JCIS 2006), October 8-11, 2006, Kaohsiung, Taiwan, ROC, pp. 1078-1081.

- [39]Tight Frame: An Efficient way for High Resolution Image Reconstruction by Raymond H.Chan. ELSEVIER Publications Feb 2004.
- [40]On Ambiguities in Super Resolution Modeling by Zhao Hong Wang and Feihu Qi-IEEE Signal Processing Letters Vol11, Nov 8, Aug 2008.
- [41] A High efficiency Super Resolution Reconstruction Algorithm from Image/Video Sequences by Chaunghai Xia.
- [42]Performance Evaluation of Super Resolution Reconstruction Methods on real World Data by A.W.M.Van Eekern, K.Schuttle, O.R.Oudegeest and L.J.Van Vliet –EURASIP Journal on Advances in Signal Processing Vol2007
- [43] High Resolution Images from low resolution compressed video by C.Andrew Segall, Rafael Molina and Aggelos K.Katsaggelo –IEEE Signal Processing Magazine May 2003